

Ambient air pollution level in the east African region based on satellite remote sensing of NO₂, CO, and Aerosol optical depth

Valérien Baharane^{1,*}, and Andrey B. Shatalov¹

¹Peoples' Friendship University of Russia, Institute of Environmental Engineering, Moscow, Russia

Abstract. This study used ten years (2013-2022) of satellite observations to assess the levels of nitrogen dioxide (NO₂), carbon monoxide (CO), and aerosol optical depth (AOD) over Eastern Africa. NO₂ vertical column density (VCD) varied between 3.17×10^{14} and 4.70×10^{14} molecules cm⁻² with a seasonal variability reaching the peak in December every year. CO mixing ratio oscillated between 95.256 ± 15.480 ppbv and 76.011 ± 5.609 ppbv and demonstrated a bimodal seasonal variability. The level of AOD fluctuated between 0.126 ± 0.070 and 0.250 ± 0.165 . Generally, the concentrations of these pollutants are comparable to the global levels, though the AOD increasing trend is an indicator of the deterioration of air quality in the east African region.

1 Introduction

Air pollution is the world's largest single environmental and health risk [1]. Although the problem of air pollution is global, its effects are more alarming for low- and middle-income countries [2]. The absence of adequate air pollution monitoring networks is often mentioned as the main cause of the slow response to tackling air pollution in those countries [3]. Therefore, most African countries still rely on solely WHO estimates.

Fast urbanization which lacks supporting infrastructures, and rapid economic growth are the main causes of the deterioration of air quality in African cities [4]. On this, is added biomass and solid fuel burning as energy sources for industries and household use. East African countries are among the countries witnessing rapid economic development, but this growth is also accompanied by environmental deterioration, especially in urban areas [5]. To enrich the knowledge of air pollution dynamics in this region, this study assessed the level of air pollution by focusing on satellite observations of NO₂, CO and AOD.

2 Material and methods

We used NO₂ from Ozone Monitoring Instrument (OMI). OMI is onboard of Aura satellite that observes the Earth at a high spatial resolution with a ground pixel of $0.25^\circ \times 0.25^\circ$. This study analysed the Level-3 daily global gridded NO₂ (OMNO2d) total tropospheric column,

* Corresponding author: vbaharane@gmail.com

for all atmospheric conditions, and for sky conditions and cloud fractions less than 30% [6]. The CO concentrations were retrieved from the Atmospheric Infrared Sounder (AIRS) repository [7]. We selected the 500 hPa pressure daytime level, which is the best representation of the ground level of the east African region since its land features range between 0 and 5895 m of altitude [8].

AOD used in this study is the Moderate-Resolution Imaging Spectroradiometer (MODIS) product. Our analysis used the Combined Dark Target and Deep Blue AOD at 0.55 microns for land and ocean, with the daily mean sampled at $1^\circ \times 1^\circ$ [9]. Ground observations of AOD were acquired from Aerosol Robotic Network (AERONET) [10]. This study uses the quality-assured level 2.0 AERONET products [11] at Bujumbura-Burundi (3.380 S, 29.384 E) and Malindi-Kenya (2.996 S, 40.194 E) stations.

Data analysis was first done by averaging daily samples to monthly and annual means. We used statistical models to analyse the time series. Furthermore, the comparison of AOD from MODIS with AERONET products was done by conducting a correlation analysis and by calculating the root mean square error (RMSE) on each grid pixel containing the AERONET station.

3 Results and discussions

Fig. 1 shows the time series for observed, trend, and seasonality plotted side-by-side with the heatmap for NO₂. The monthly average tropospheric NO₂ VCD ranged from 3.17×10^{14} to 4.70×10^{14} molecules cm⁻², observed in April 2020 and December 2013, respectively. NO₂ displayed a pronounced seasonality with peaks in December and valleys in March-April of every year. The monthly values represented by the heatmap displayed that, in general, the NO₂ VCD increased from May to December before a decrease to its minimum value in April every year.

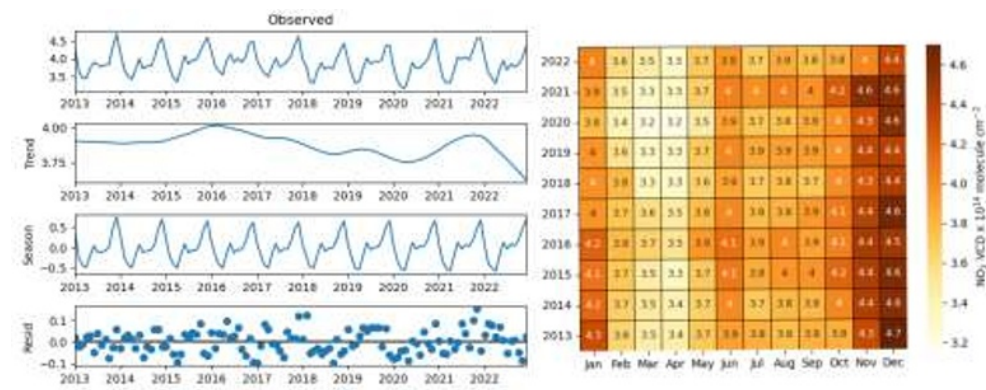


Fig. 1. Time series (left) of NO₂ VCD ($\times 10^{14}$ molecules cm⁻²), and heatmap (right) for monthly values.

It can be noted that the seasonal variability of NO₂ is linked with the local weather patterns [12] with dry seasons corresponding to higher pollution levels. During the study period, NO₂ VCD did not demonstrate a significant trend as proved by a non-parametric Mann Kendall (MK) trend test ($p = 0.886$, $\tau = -0.009$). However, it decreased from 2016 to 2020 (Fig.1).

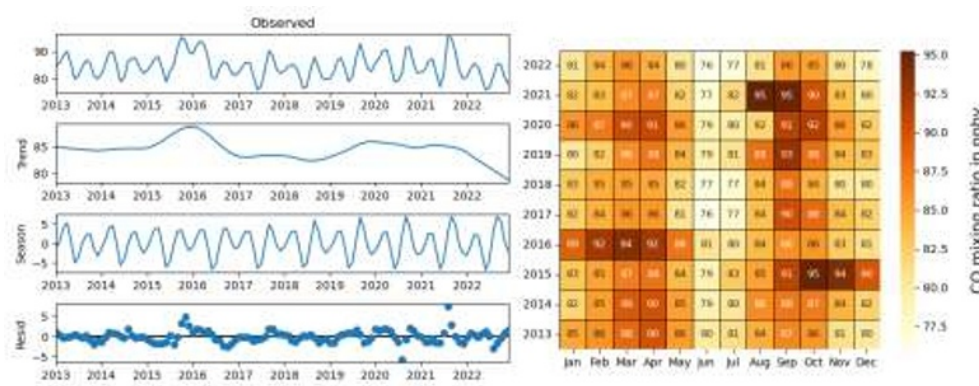


Fig. 2. Time series plots of CO mixing ratio (left), and heatmap (right) for monthly values.

Carbon monoxide exhibited a two-peak seasonality with a higher peak in September-October and a lower one in March-April of every year (Fig. 2). The monthly average of CO mixing ratio varied between 95.256 ± 15.480 ppbv and 76.011 ± 5.609 ppbv observed in August 2021 and June 2022, respectively. There is no significant trend observed (MK: $p = 0.078$, $\tau = -0.109$) but, since 2016, CO concentration decreased. The drop in CO concentrations is a global trend since 2000 and is attributed to the decline in anthropogenic emissions in developing countries and the reduction of biomass burning, particularly in African countries [13].

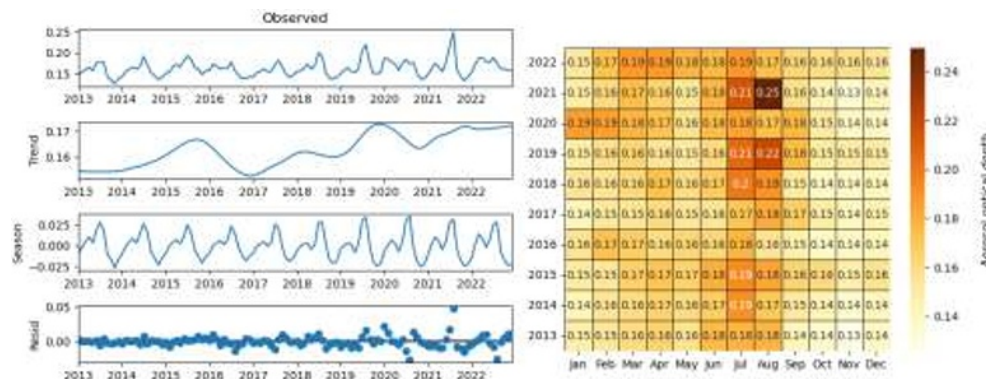


Fig. 3. Time series plots of AOD (left), and heatmap (right) for monthly values.

Fig. 3 presents the monthly variability of AOD. The maximum and minimum values were 0.250 ± 0.165 and 0.126 ± 0.070 , respectively observed in August 2013 and November 2021. These values are comparable to the globally observed AOD [14]. AOD increased steadily during the study period (MK: $p = 0.042$, $\tau = 0.126$). The increase in AOD indicates the degradation of air quality in the East African region.

Analogous to NO₂ and CO, AOD exhibited seasonal variability with a peak in August and a valley in November. The correlation analysis demonstrated that the satellite observations best fit the ground monitoring for AOD (Fig. 4). The RMSE of MODIS against AERONET products at Bujumbura and Mbita sites were 0.218 and 0.073, respectively.

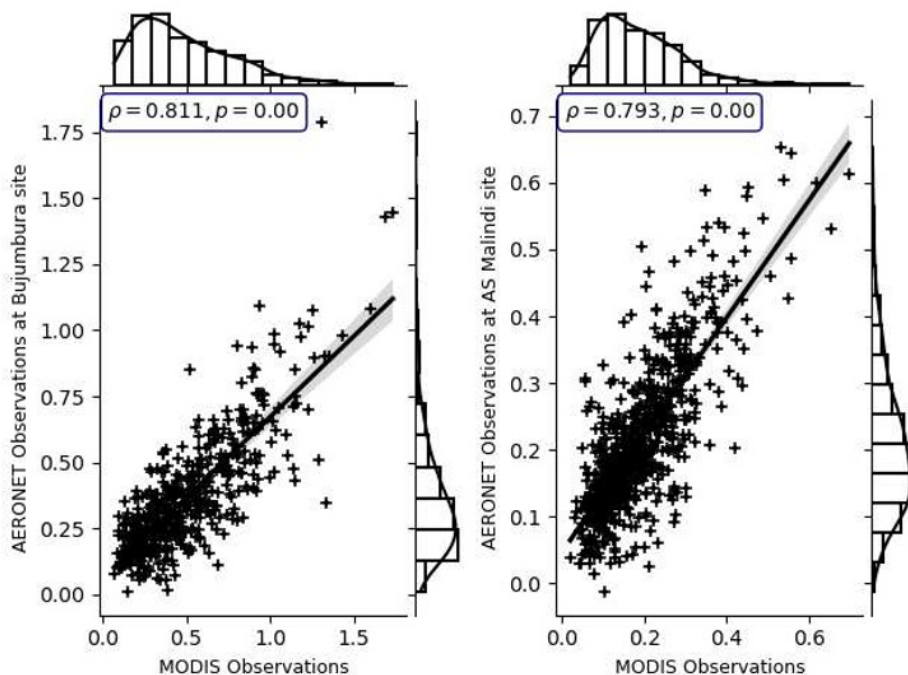


Fig. 4: Correlation between AIRS and AERONET observations

4 Conclusions

This study investigated the level of atmospheric pollution in the East African region by using ten-year (2013-2022) satellite observations. The Statistical analysis demonstrated that NO_2 VCD are higher in December and lower in April every year. In contrast to NO_2 and CO, AOD increased all over the study period. Generally, the concentrations of these pollutants were similar to the global levels, though the increase in the AOD may be interpreted as an indicator of the deterioration of ambient air quality in the region. Therefore, there is a need for in-situ monitoring for the better characterization of air pollution levels in the East African region.

We thank the AERONET principal investigators, co-investigators, and their staff at Bujumbura and Malindi sites for establishing and maintaining the sites used in this research.

References

1. R. Fuller, P. J. Landrigan, K. Balakrishnan, G. Bathan, S. Bose-O'Reilly, M. Brauer, et al., *Lancet Planet. Heal.* **6**, e535 (2022)
2. UNEP, United Nations Environ. Program. 19 (2019)
3. A. K. Amegah and S. Agyei-Mensah, *Environ. Pollut.* **220**, 738 (2017)
4. J. Keel, K. Walker, and P. Pant, *Clean Air J.* **30**, 1 (2020)
5. A. Mazzeo, M. Burrow, A. Quinn, E. A. Marais, A. Singh, D. Ng'ang'a, M. J. Gatari, and F. D. Pope, *Atmos. Chem. Phys.* **22**, 10677 (2022)
6. N.L. Lamsal, N.A. Krotkov, A. Vasilkov, S. Marchenko, W. Qin, Z. Fasnacht, J. Joiner, S. Choi, D. Haffner, W. H. Swartz, B. Fisher, and E. Bucsela. AGU Fall Meeting Abstracts, A13K-2976 (2019)

7. AIRS project, Goddard Earth Sci. Data Inf. Serv. Cent. (GES DISC) (2019)
8. L. L. Kebacho, *Meteorol. Atmos. Phys.* **134**, 1 (2022)
9. S. Platnick, K. Hubanks, K. G. Meyer, and M. D. King, Goddard Sp. Flight Cent. (2015)
10. Z. Li, C. Li, H. Chen, S. C. Tsay, B. Holben, J. Huang, B. Li, H. Maring, Y. Qian, G. Shi, X. Xia, Y. Yin, Y. Zheng, and G. Zhuang, *J. Geophys. Res. Atmos.* **116**, 0 (2011)
11. D. M. Giles, A. Sinyuk, M. G. Sorokin, J. S. Schafer, A. Smirnov, I. Slutsker, T. F. Eck, B. N. Holben, J. R. Lewis, J. R. Campbell, E. J. Welton, S. V. Korkin, and A. I. Lyapustin, *Atmos. Meas. Tech.* **12**, 169 (2019)
12. S. E. Nicholson, *Rev. Geophys.* **55**, 590 (2017)
13. A. Singh, D. Ng'ang'a, M. J. Gatari, A. W. Kidane, Z. A. Alemu, N. Derrick, M. J. Webster, S. E. Bartington, G. N. Thomas, W. Avis, and F. D. Pope, *Environ. Res. Commun.* **3**, 75007 (2021)
14. Q. Bourgeois, A. M. L. Ekman, J. B. Renard, R. Krejci, A. Devasthale, F. A. M. Bender, I. Riipinen, G. Berthet, and J. L. Tackett, *Atmos. Chem. Phys.* **18**, 7709 (2018)